Paper C:9
Hidrography Committee
Sess. Computers in Fishery Research

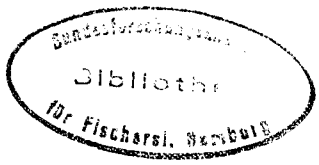

INFRARED IMAGE INTEGRATION FROM METEOSAT AND NOAA SATELLITES USING CROSS CORRELATION TECHNIQUES

Authors: **J. M. Cotos*, J. A. Triñanes*, C. Bóveda*, J. E. Arias****

University of Santiago.
15706 Santiago de Compostela. Spain.

*** Applied Physics Department.**

**** Electronics and Computer Sciences Department**

A paper presented at the 81st Statutory Meeting of the International Council for the Exporation of the Sea (ICES). Dublin, Ireland. 23 September - 1 October, 1993.

ABSTRACT

We present one of the low level tasks of an expert system to detect and monitor upwelled areas in East Atlantic. The system integrates NOAA and Meteosat infrared images to obtain big areas of water with well known temperature. This provides us large scale thermal maps, and gives a overall view of the situation in the ocean.

The first step begins with a registration of both images to the same mercator projection. We estimate SST from NOAA image using split-window algorithms and relate it with gray level values of the Meteosat image via a regression line. By means of cross correlation techniques, we are able to extract the training samples to get the regression line.

This algorithm will also be used to calibrate Meteosat images in such way that we will be able to know the temperature in parts of the Indian Ocean that we have not NOAA images. This knowledge would be very interesting to the tuna fisheries that take place near Madagascar.

1.- INTRODUCTION

The study of upwelling on the West Coast of the Iberian peninsula presents a relevant economic importance owing to the direct relation the coast towns maintain with fishing and shellfish catching. Studies carried out by Fiuza (1) show that the behaviour of the sardine in its biological cycles is directly marked by the presence or absence of this event. In the same way, studies realized by Blanton (2) also show a close relation between the highest production of mussels and the presence of upwelling in the Galician estuaries, because it provides the basic nutrients which start primary and secondary production.

The study of the evolution of upwelling is normally realized (3) by means of images obtained from the NOAA polar satellites, but it may be completed with images obtained in the infrared range by the meteorologic Meteosat-5, because a single satellite does not normally satisfy the spacial or temporal requirements necessary for the study of a concrete process. Thus, the high temporal resolution of satellite Meteosat-5 allows us to observe zones which have been covered by clouds and have later cleared up during the day.

In this paper we are introducing the methodology necessary to calibrate the digical levels obtained in the infrared range by means of the Meteosat-5 satellite and the data about temperature obtained by the NOAA satellite. This technique will constitute a low level task for an expert system which will detect and monitor the areas of upwelling that exist in a certain image, and will enable us to estimate the temperatures from Meteosat-5 in areas which we cannot possibly get from our reception station with the NOAA satellites. This happens with the Indic Ocean at the level of the Madagascar Island, where important tuna fish catches take place.

2.- IMAGES

We are integrating two images, one from the geostationary meteorologic satellite Meteosat-5 and another from the polar satellite NOAA-11, both obtained on July 16th, 1993, corresponding to the West Coast of the Iberian Peninsula and in particular to an area centered in 41N, 10:18W, with an extension of approximately 256 x 512 km. This area is briefly represented in figure 1.

The firts image was obtained in high resolution mode (800 x 800 pixels), 5x5 km per pixel, and corresponds to the infrared channel of Meteosat-5 (see table I). The second one, the higher resolution image, belongs to NOAA-11, and has been geometrically corrected to a rectangular projection. We have extracted the superficial sea temperatures from the thermic infrared channels 4 and 5 belonging to the AVHRR sensor between 10.5 and 12.5 micras (see table I).

In order to do this, we have used a split window method (4). In table II we can see the calibration parameters of the black body, as well as the slopes and intercepts of the visible channels.

SATELLITE	DATE / TIME	CHANNEL	BITS/PIXEL
Meteosat-5	15-June-1993 / 15:00	INFRARED - 10.5-12.5	8
NOAA 11 AVHRR	15-June-1993 / 16:26	FOUR - 10.5-11.5 FIVE - 11.5-12.5	10

Table I. Description of the images used

CHANNEL	SLOPE	INTCPT	DEEP SPACE	BLACK BODY RADIANCE	TERMOMETER	AVERAGE TEMP FOR BLACK BODY
1	0.09060	-3.73	39.9		1	299.96
2	0.08270	-3.39	39.6		2	307.00
3	- 0.00150	1.48	989.4	691.8	3	306.00
4	- 0.17845	177.21	993.1	432.0	4	316.00
5	- 0.18253	181.95	996.8	368.0		

Table II. Results of NOAA-11 calibration to extract SST

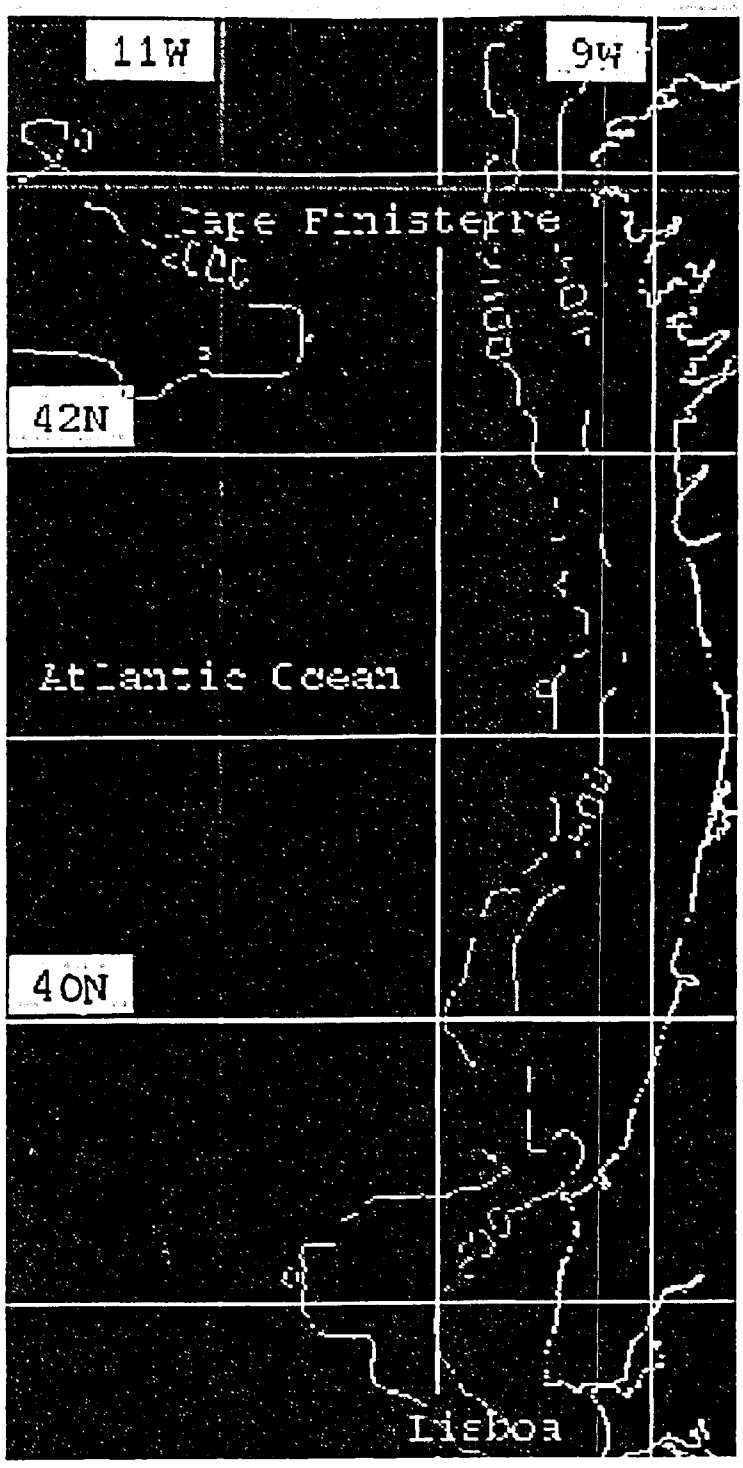

Fig. 1 WEST COAST OF THE IBERIAN PENINSULA

3.- METHODOLOGY

We will try to correlate the digital levels presented by satellite Meteosat-5 with the temperatures obtained from NOAA-11. In order to do this, we will look for training areas that coincide in both images and which will enable us to obtain pairs of the type digital level-temperature and estimate a regression line. To estimate these common areas we have decided to use correlation statistics methods between pairs of images (5).

The first step consists in trying to make the spatial resolutions in both satellites equal. Owing to the fact that the spatial resolution of the AVHRR sensor in the NOAA satellites is of 1.1 km per pixel in the NADIR, and the resolution of the infrared sensor in the Meteosat-5 is of 5 km per pixel also in the NADIR, we enlarge the image from Meteosat-5 five times, obtaining a resolution of 1km per pixel. So as not to vary the digital levels in this enlargement of the image, we have interpolated the method of the nearest neighbour (6).

In general, the sea areas presented in a reduced part of the image, as is the case, present their grey levels corresponding to the sea in a very small range of the hystogram, owing to the small variation in the temperature range (nearly 4 or 5 degrees centigrade), so that the aparent noise of high frequency is higher than when the global image is considered. As our image has been enlarged, this noise is even higher, so that in order to obtain homogeneous areas, we have subjected it five times to a consecutive filtering of the mediam filter (7). This allows us to see homogeneous areas in it, which are identifiable with those appearing in the thermic map.

The following step in the search for training areas is to correct the Meteosat-5 image with respect to that of the NOAA, so that pixels with identical subindexes in the image correspond to sea areas sufficiently close together. With this aim, we use a wrapping method (8) by selecting 10 perfectly known points along the coast and carrying out a bilinear interpolation according to equation $a+bx+cy+dxy$.

Once both images are georefferencially identical we choose the training areas through cross correlation statistical methods.

The method we are going to describe is based on the calculation of the cross-correlation coefficient between different windows belonging to the image from NOAA satellite, which we will call principal, and the other image (the one belonging to Meteosat-5 sat.). We will suppose that there have been no rotations, because the method is only sensitive to the translations according to the X or Y axis.

We define the cross-correlation coefficient of two random variables X and Y as (9):

$$\rho = \frac{\mathrm{cov}(x,y)}{\sqrt{\mathrm{var}(x)\,\mathrm{var}(y)}} \qquad (1)$$

We will divide our principal image in size 32x32 cuadrants, and will be looking for similitudes in a window situated in the second image of 64x64. We will have 32x32 possible movements according to the two axis so that the position of the calculated peak ρ will indicate which the movement suffered by the upwelling is. If we note the cuadrant in the first image by $f(x,y)$, and the moved cuadrant by $g(x+\varepsilon,y+\eta)$, the amount (ε,η), ec.1 will become,

$$\rho(\varepsilon,\eta) = \frac{\mathrm{cov}(f(x,y), g(x+\varepsilon, y+\eta))}{\sqrt{\mathrm{var}[f(x,y)]\,\mathrm{var}[g(x+\varepsilon, y+\eta]}} \qquad (2)$$

where,

$$VAR[f(x,y)] = \frac{1}{R}\iint \left(f(x,y) - \bar{f}\right) P_{f(x,y)}\, dx\, dy \qquad (3)$$

f, is the expected value in the window as we call it in stadistics:

$$\bar{f} = E[f(x,y)] = \frac{1}{R}\iint f(x,y)\, P_{f(x,y)}\, dx\, dy \qquad (4)$$

$$var[g(x+\varepsilon, y+\eta)] = \frac{1}{R}\iint \left(g(x+\varepsilon, y+\eta) - \bar{g}(\varepsilon,\eta) \right) P_{g(x+\varepsilon,y+\eta)}\, dx\, dy \qquad (5)$$

$$\bar{g}(\varepsilon,\eta) = \frac{1}{R}\iint g(x+\varepsilon, y+\eta)\, P_{g(x+\varepsilon,y+\eta)}\, dx\, dy \qquad (6)$$

As we have already calculated the expected values in both windows, we use the ecuation (6) to calculate the co-variance between both functions:

$$\begin{aligned} &cov[f(x,y), g(x+\varepsilon, y+\eta)] = \\ &= E[f(x,y)\cdot g(x+\varepsilon, y+\eta)] - E[f(x,y)]\cdot E[g(x+\varepsilon, y+\eta)] \end{aligned} \qquad (7)$$

$$E[f(x,y)\cdot g(x+\varepsilon, y+\eta)] = \frac{1}{R}\iint f(x,y)\cdot g(x+\varepsilon, y+\eta)\cdot Pc_{f,g}\, dx\, dy \qquad (8)$$

The concept of *overall or conditional probability* appears here associated to the random variables, Pc_{fg} which is the probability that once the grey level f(x,y) has appeared in the first image, we will obtain the level g(x+ε,y+η) in the second one, which is defined as:

$$Pc_{f,g} = \lim_{n\to\infty} \frac{n_{12}}{n_1 + n_{12}} \qquad (9)$$

where n is the number of points in the image, n_1 the number of times that the level of grey f(x,y) has appeared in the first image and n_{12} the number of occasions on which, once f(xy) has already appeared in the first image, we obtain g(x+ε,y+η) in the second. Maximum ρ relates one square belonging to the firt image with another in the second one.

Once this process has been followed, we obtain pairs of points of the type digital level-temperature by working out the average of the 25 neighbouring values existing in the centre of each window. We have decided on this number of values (a 5x5 square concentric with the window), because the training area found represents a 32x32 window. This parameter is susceptible to be changed.

The data thus obtained have been adjusted by means of a lineal and exponential regression as we can see in figure 2. Here, the grey levels (equivalent to radiance) obtained in the image of the Meteosat -5 have been represented on the Y axis, while on the X axis we have represented the temperatures obtained from the image of the NOAA-11 multiplied by a factor of 10.

Both types of adjustment are so similar that it is practically impossible to differenciate them in figure 2, and both present a regression coefficient of 0.47.

This result may not seem the best possible one, but we have to consider the great spatial difference that both images presented.
For this reason, and owing to the great number of samples obtained (350) for the calculation of the regression, we consider that this result is good enough to estimate temperatures in the range of 12 to 15 degrees centigrade starting with the Meteosat-5 images obtained in high resolution inside our laboratory.

4.- CONCLUSIONS

The method developed allows us to obtain a thermic map of low spatial resolution generated from a Meteosat image and from a NOAA image. The main handicap we have been confronted with is the limited thermic margin presented by the image used to obtain the regression line, because we cannot conclude that the line obtained should be valid in a range superior to 10 degrees centigrade (10 and 20). We might possibly obtain higher results with searching areas of higher pairs. This would imply a higher computering cost because correlation methods are excessively slow. We consider that the regression coefficient obtained is valid because of the different spatial resolutions presented by the images.

This method will allow us to carry out a study of Iberian upwelling starting with low resolution images and going on to the group's investigation line. It constitutes one of the low level tasks for an expert system designed to automatically determine the presence or absence of upwelling at different points of the coast. At the same time, it enables us to extrapole the result obtained to calculate temperatures in areas where we cannot get them from polar satellites.

Thus, we are able to design thermic maps in areas of high comercial interest such as the Indic ocean near Madagascar, where important tuna fish catches occur.

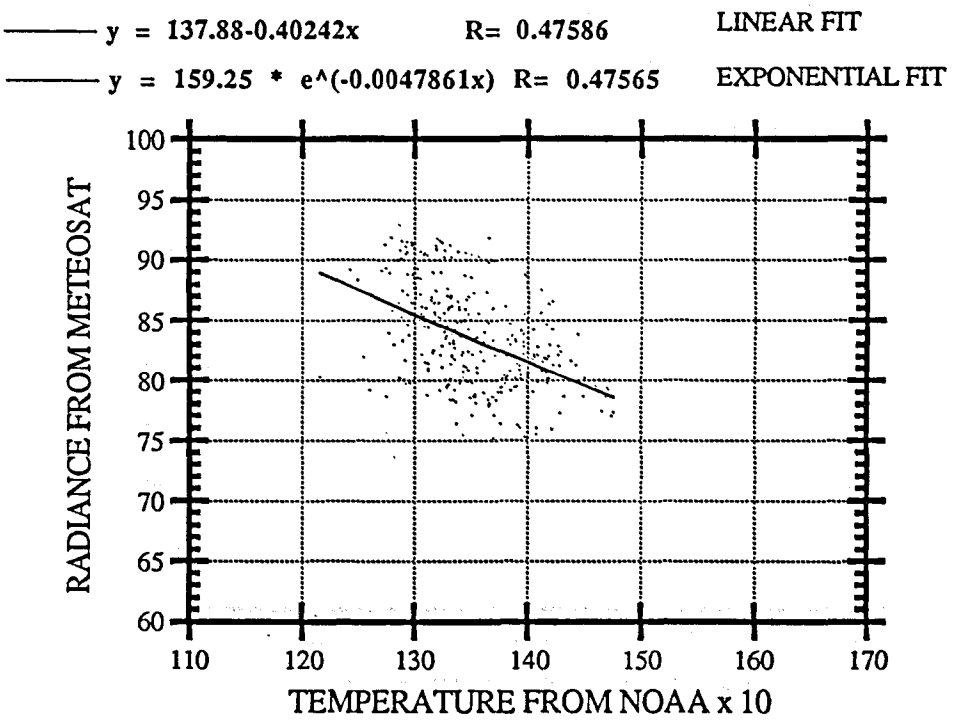

Figure 2. Radiance versus temperature (in Celsius x 10) and its regression lines

5.- REFERENCES

1.- A. F. Fiúza, M. E. Macedo, M. R. Guerriro. "Climatological Space and Time Variation of the Portuguese Coastal Upwelling". Oceanologica Acta. Vol 5, nº1, pp. 31-39. 1982.

2.- J. O. Blanton, K. R. Tenore, F. Castillejo, L. P. Atkinson. "The Relationship of Upwelling to Mussel Production in the Rias on the Western Coast of Spain". Journal of Marine Research, 45, pp. 497-511. 1987.

3.- P. C. Fiedler, G. B. Smith, R. M. Laurs. "Fisheries Applications of Satellite Data in the Eastern North Pacific". Marine Fisheries Review. Nº 46, pp. 1-13. 1984.

4.- E. P. McClain, W. G. Pichel, C.C. Walton. "Comparative Performance of AVHRR-Based Multichannel Sea Surface Temperatures". Journal of Geophysical Research. Vol 90, nº C6, pp 11587-11601. 1985.

5.- W. J. Emery, A. C. Thomas, M. J. Collins."An Objective Method for Computing Surface Velocities from Sequential Infrared Satellites Images". Journal of Geophysical Research, pp. 12865-12878, vol 91, nº C11, November,15 1986.

6.- Willian K. Pratt. "Digital Image Processing". Ed. John-Willey&Sons, 1978.

7.- Paul M. Mather. "Computer Processing of Remotely-Sensed Images. An Introduction.". Ed. John-Willey&Sons, 1987.

8.- Chuvieco E. "Fundamentos de Teledetección Espacial". Ed. Rialp, Madrid 1990.